Macromolecules

pubs.acs.org/Macromolecules Article

9,9-Dimethyl Dihydroacridine-Based Organic Photocatalyst for Atom Transfer Radical Polymerization from Modifying "Unstable" Electron Donor

Yiming Liu, Qi Chen, Yujie Tong, and Yuguo Ma*

Cite This: *Macromolecules* 2020, 53, 7053−7062 Read Online

ACCESS | Metrics & More | Article Recommendations | Supporting Information

ABSTRACT: Organic photocatalytic atom transfer radical polymerization (ATRP) has recently become a research highlight. Organic photocatalysts based on phenothiazine, phenoxazine, and phenazine have been reported and exhibited remarkable performance. All of those structures contain two heteroatoms, which makes the oxidative state (i.e., the radical cation) of the photocatalysts stable enough to complete the catalytic cycle. However, despite the similar structure, 9,9-dimethyl dihydroacridine (DHA) was rarely used for constructing photocatalyst due to its unstable oxidative state. DHA is a weak electron donor that was widely applied in blue-emitting thermally activated delayed fluorescence (TADF) molecules. Its weaker electron-donating ability will contribute to a higher energy level of the excited state. Also, the higher oxidation potential of its radical cation will contribute to better controllability due to fast reversible dormancy. In this study, we found that substitution on the active sites of DHA could make it stable enough to be the donor part of a donor−acceptor (D−A)-type photocatalyst for ATRP. Moreover, chemical modification is necessary for both stabilizing the radical cation and improving the controllability in the polymerization process. Further modification was made to construct a rapid equilibrium between initiation and reversible dormancy, and polymerization with quantitative initiator efficiencies was achieved with a polydispersity of 1.14. It is notable that such modification can probably apply to different kinds of electron donors, and various organic chromophores could thus be applied to construct organic photocatalyst with superior performance.

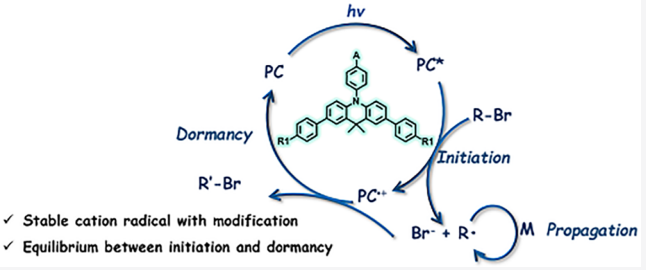

INTRODUCTION

The idea of photochemistry was proposed in the early 19th century,[1] and photocatalysis has been well developed so far, both in the synthesis of small molecules and in polymerization. Numerous systems have been designed for photocontrolled atom transfer radical polymerization (photo-ATRP). In living ATRP system, a matched rate of initiation and reversible dormancy is the key of controllability and achieving living polymerization.[2] According to the oxidative quenching mechanism[3] (Figure 1a), after the initiator is reduced by photocatalyst, the generated radical cation could oxidize the propagating chain radical to dormant species (R−X). Therefore, it is necessary for a photocatalyst to possess a stable oxidative state. The rate of initiation is determined by the reducibility and concentration of excited photocatalyst, while the reversible dormancy rate is determined by the oxidative potential and stability of the radical cation.[4,5] As shown in Figure 1b and 1c, for some photocatalysts, such as metal complexes and organic photocatalysts with heavy atoms, the ISC (intersystem crossing) rate is fast. Thus, the radioactive decay and ISC processes are favored for S_1, and the generated long-lived T_1 would prefer the PET (photoinduced electron transfer) process. However, for most heavy-atom-free organic photocatalysts, the PET and ISC processes are too slow to compete with radioactive decay of S_1, that is, in a photocatalytic system, there is a competition between different pathways of decay, including radiative decay, a PET process, and other types of nonradiative decay. Also, it is shown that both a longer lifetime and stronger reducibility of the excited state would contribute to efficient PET. If the rates of PET and other decay processes were competitive or the rate of PET was much faster, participation and even domination of the singlet states in catalysis is possible. Thus, this process could probably be initiated by both singlet and triplet excited states.[6,7]

Transition metal complexes have been widely applied in photo-ATRP for their long lifetime of the excited states and chemical stability.[8−17] Once excited, transition metal complexes could reach the triplet excited state rapidly due to efficient spin−orbit coupling (SOC). However, metal contamination must be avoided in some areas, such as biological and magnetic

Received: February 15, 2020
Revised: July 1, 2020
Published: August 5, 2020

https://dx.doi.org/10.1021/acs.macromol.0c00377
Macromolecules 2020, 53, 7053−7062

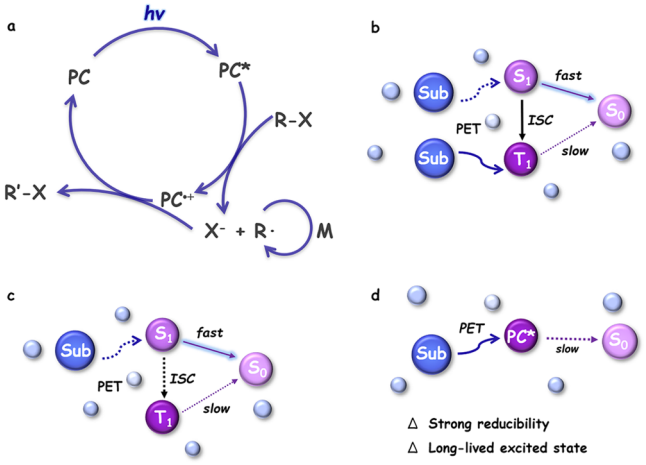

Figure 1. (a) Oxidative quenching mechanism of photocontrolled polymerization, and different decay pathways of excited photocatalysts in solution. Sub is the representation of substrate. (b) PCs with fast ISC, such as metal complexes and heavy-atom-containing organic PCs. (c) For some heavy-atom-free organic photocatalysts, PET and ISC processes are too slow to compete with radioactive decay of S_1. (d) More general illustration of the photoredox catalyst. Different states of the photocatalyst are represented by purple spheres, substrate is represented by a violet blue sphere, and solvent is represented by a light blue sphere.

materials.[18] Considering that, an organic photocatalyst (PC) has been drawing wider attention as it may be the key to extend application ranges of the photocatalyst. However, for most heavy-atom-free organic PCs, the ISC efficiency is generally very low and their singlet excited state lifetime is short and not efficient enough for electron transfer in solvent at room temperature. In comparison, metal complexes usually possess a fast ISC rate and the lifetime of resultant triplet excited state is much longer (greater than or equal to several microseconds)[19] which is of benefit for further reaction. There are ways to improve their performance for photo-ATRP, such as increasing photocatalyst loading, enhancing absorption of the photocatalysts, prolonging the lifetime, and improving the reducibility of their excited state. Over the past decades, design of organic PC for controlled polymerization has drawn wide attention. Also, computation-assisted design and screening of organic PCs has provided a novel research method more recently.[20−22] Electron-deficient organic dyes, such as thioxanthone,[23] benzophenone,[23] fluorescein,[24] and its derivatives,[25] combining amine could mediate photo-ATRP through a reductive quenching mechanism. Also, organic dyes such as PAHs (polycyclic aromatic hydrocarbons),[26,27] thienothiophene,[28] and pyridine-diketopyrrolopyrrole[29] have been used to mediate photocontrolled polymerization through an oxidative quenching mechanism. Recently developed organic PCs based on phenoxazine,[30,31] phenazine,[4,6,32,33] and phenothiazine[34−36] derivatives have been proven to be successful prototypes for photo-ATRP. Well-controlled photo-ATRP was performed under light irradiation. All of those structures contain two heteroatoms, which makes the oxidative state (i.e., the radical cation) of the photocatalysts stable enough to complete the catalytic cycle. However, the library of photocatalysts structure is limited according to this standard. Chemical structures bearing an unstable oxidative state could also be used as well-performing photocatalysts with proper modification.

In 2011, organic thermally activated delayed fluorescence (TADF) dyes were developed by Adachi's group.[37] Organic TADF molecules generally bear a donor−acceptor (D−A) structure with charge-transfer (CT) characteristic excited states. Minor overlap of singly occupied molecular orbitals (SOMOs) in the CT excited states decrease ΔE_{ST} effectively, which make reverse ISC (RISC) a thermally activated process. Thus, short-lived (nanoseconds) prompt fluorescence and longer-lived (microseconds) delayed fluorescence can be detected in these systems.

Inspired by the designing strategy of TADF molecules,[38−42] we reasoned that D−A (donor−acceptor) structures with separated HOMOs and LUMOs will prolong the excited state lifetime of the organic photocatalyst by reducing the SOMOs overlap in the CT (charge transfer) characteristic excited state. Also, it was proposed that the intramolecular CT excited state will benefit photocatalysis due to a reduction of the fluorescence and improvement of the PET rate.[32] The energy of the CT

Scheme 1. Molecular Structures of DHA-Based Photocatalysts

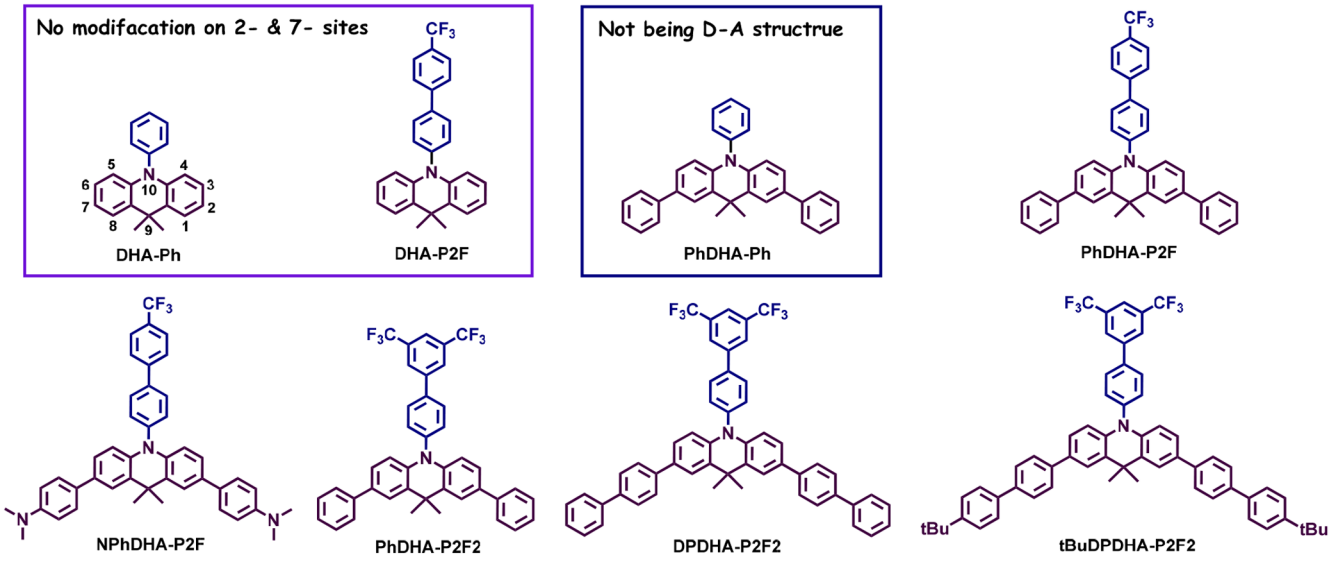

https://dx.doi.org/10.1021/acs.macromol.0c00377
Macromolecules 2020, 53, 7053−7062

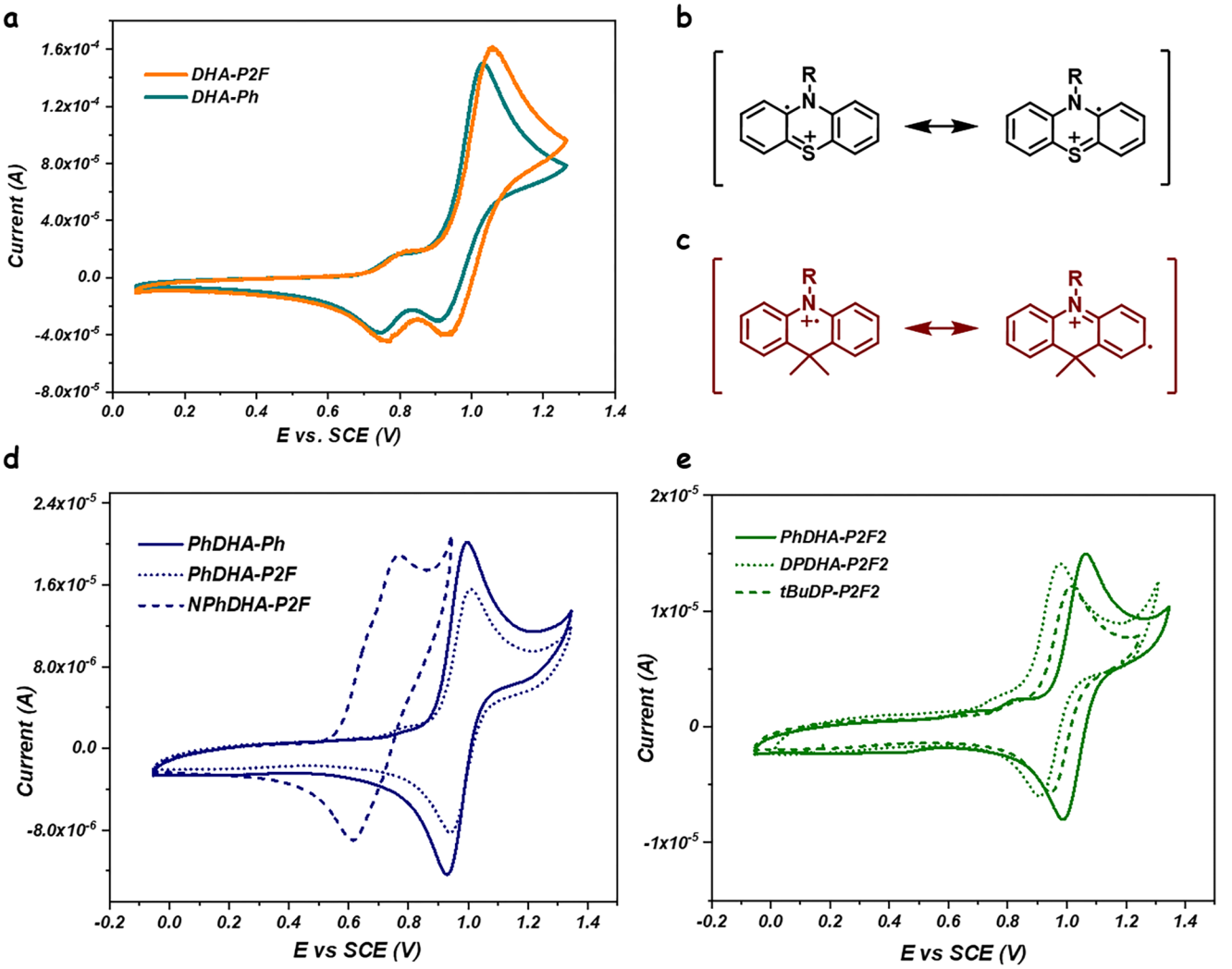

Figure 2. (a) Cyclic voltammetry curve of DHA-Ph and DHA-P2F, 1 mg/mL in MeCN. (b) Resonant structures stabilizing the radical cation of phenothiazine. (c) 2- and 7-sites of the DHA radical cation are unstable with only one heteroatom. (d and e) Cyclic voltammetry curve of substituted photocatalyst, 1 mg/mL in *N*,*N*-dimethylacetamide (DMA).

excited state can be estimated by the energy level of the frontier orbitals, so a D−A structured molecule with a weak donor can possess a CT excited state with a high energy level. Also, the strong oxidation potential of its radical cation could contribute to better controllability due to fast reversible dormancy. 9,9-Dimethyl dihydroacridine (DHA) is a weak electron donor that was widely applied in blue-emitting TADF molecules.[43−49] However, it was rarely used to construct a photocatalyst due to its unstable oxidative state[50] and weak absorption. Here, we reason that a well-performing photocatalyst based on DHA can be attained through appropriate chemical modification. A series of organic photocatalysts based on DHA for photo-ATRP under visible light was designed, and rational chemical modification was proved to be a solution to design organic photocatalyst for stabilizing the radical cation and increasing the absorption of visible light. Coincidently, Miyake et al. reported a new series of photocatalysts based on 9,9-dimethyl dihydroacridine, which performed well in the controlled polymerization of acrylate monomer under 365 nm irradiation. Also, a well-defined triblock polymer was synthesized. Addition of LiBr and a continuous flow reactor were essential to improve the controllability.[51] It is necessary to state that our work aims to construct a D−A type of photocatalyst by rationally modifying the "unstable" electron donor and performing controlled ATRP under visible light. Notably, this method may be applicable to other types of donors to extend the scope of organic photocatalysts.

RESULTS AND DISCUSSION

Molecular Design. To elucidate how a substituent would affect the catalytic performance of the DHA-based photocatalyst, we designed molecules as in Scheme 1. Molecules without modification on the 2- and 7-sites of DHA (DHA-Ph and DHA-P2F) and PC (PhDHA-Ph) not having a D−A structure were synthesized for reference. To prolong the lifetime of the excited state, phenylene was introduced as π-spacer between the donor and the acceptor for reducing the overlap of the SOMOs. The electron-withdrawing ability was adjusted by the number of trifluoromethyl groups in the acceptor. The precursors were synthesized by Buchwald−Hartwig cross-coupling, and then the DHA part was modified with different substituents on the 2- and 7-sites (SI S2).

Electrochemistry. According to the mechanism of photo-ATRP, the oxidative photocatalyst, i.e., the radical cation, reacts with the propagating chain to induce the reversible dormancy.[4]

https://dx.doi.org/10.1021/acs.macromol.0c00377
Macromolecules 2020, 53, 7053−7062

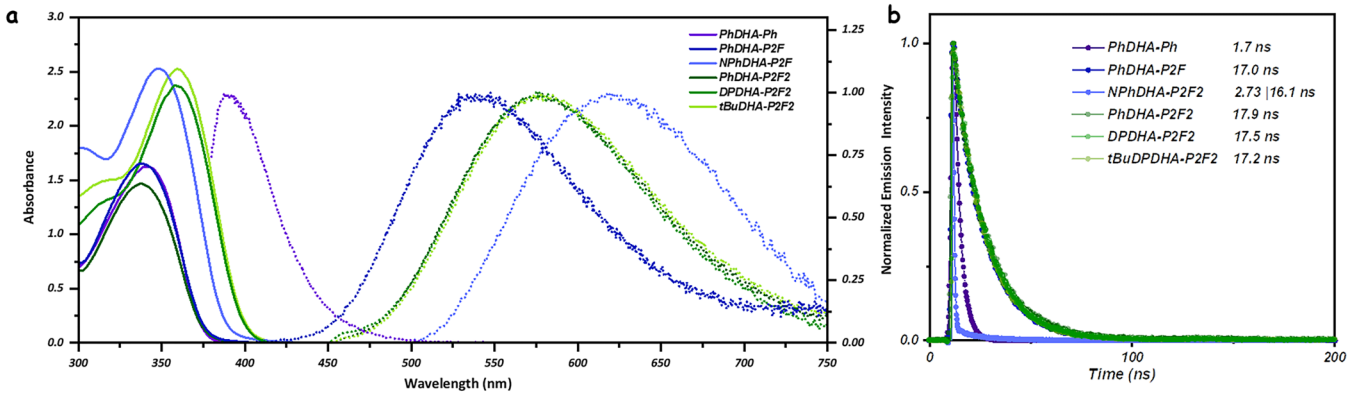

Figure 3. (a) Absorption and emission and (b) lifetime spectra of photocatalysts. Samples were dissolved in DMA (5.7×10^{-5} M). Emission and lifetime were measured with deoxygenation through three freeze−pump−thaw cycles.

Table 1. Summary of the Electrochemical and Photophysical Properties of the Photocatalysts

PC	λ_{max} (nm)	Abs.$_{max}$	τ (ns)	$E_0(PC^{\bullet+}/PC^*)^c$ (V vs SCE)	$E_0(PC^{\bullet+}/PC)$ (V vs SCE)
PhDHA-Ph	341	1.62	1.7[a]|1.6[b]	−2.27	0.96
PhDHA-P2F	338	1.65	17.0[a]|12.5[b]	−1.76	0.97
NPDHA-P2F	348	2.53	2.7,[a] 16.1[a]|1.6[b], 8.4[b]	−1.81	0.69
PhDHA-P2F2	338	1.47	17.9[a]|13.0[b]	−1.60	1.02
DPDHA-P2F2	358	2.37	17.2[a]|12.8[b]	−1.69	0.94
tBuDPDHA-P2F2	360	2.52	16.8[a]|12.6[b]	−1.65	0.98

[a]Samples were deoxidized through three freeze−pump−thaw cycles. [b]Samples were measured without deoxygenation. [c]The redox potential of the excited state was calculated according to the onset wavelength of the emission spectra.

Thus, first, the electrochemical stability of DHA-Ph was tested. The cyclic voltammetry (CV) curves of DHA-Ph and DHA-P2F are nearly irreversible (Figure 2a), suggesting that the oxidative state of DHA is unstable. Different from phenothiazine,[52,53] DHA has only one heteroatom; thus, a positive charge cannot be stabilized by delocalization on the additional heteroatom (Figure 2b and 2c). The main oxidative peak at 1.2 V vs SCE was attributed to formation of radical cation DHA$^{\bullet+}$−R. Two peaks appeared during the cathodic sweep process, corresponding to reduction of two species. It was caused by the rapid dimerization of DHA$^{\bullet+}$−R, that is, intermolecular C−C bond formation between the 2- and the 7-sites. Further, the dimeric species caused another oxidative peak at 0.8 V vs SCE.[50] The distribution of the radical on the 2- and 7-carbons causes instability of the oxidative state (Figure 2c). Thus, it is necessary to make proper modification on the 2- and 7-positions to inactivate them. Thus, a phenyl or biphenyl substituent was introduced to decrease the spin density of the 2- and 7-positions to improve the stability of the single-electron-oxidized DHA (Scheme 1: PhDHA-Ph, PhDHA-P2F, NPhDHA-P2F, PhDHA-P2F2, DPDHA-P2F2, and tBuDHA-P2F2). As expected, molecules with a phenyl or biphenyl substituent have a much more stable radical cation, which can be seen from the reversible CV curves (Figure 2d and 2e).

Photophysics. As shown in Figure 3a, the emission spectra of PhDHA-P2F and PhDHA-P2F2 are broad and featureless, which is typical of the CT excited state. Compared with PhDHA-Ph, PhDHA-P2F and PhDHA-P2F2 exhibit a red shift in the emission spectra due to the electron-withdrawing ability of the electron acceptor attaching to the nitrogen atom, which can be explained by the decreased LUMO energy level of the molecules of D−A type (vide infra). Also, with the increase of electron-withdrawing ability in the acceptor, the emission exhibits a further red shift. Most importantly, the excited state lifetime of the D−A structured molecules was remarkably prolonged (Figure 3b). The nearly orthogonal dihedral angle between the donor and the acceptor results in a small overlap between the HOMO and the LUMO. It also causes little overlap between the SOMOs of the CT characteristic S_1 state, thus decreasing the rate of radiative decay (see at the Computational Results and SI S8). However, for all of the PCs except NPhDHA-P2F, the excited states decay in a single-exponential way. The lifetime of the excited state was tens of nanosecond, which differs from the delayed fluorescence of the TADF molecules. This might be caused by the large ΔE_{ST} (vide infra) and spin-forbidden transition.

The absorption profile of the photocatalyst is mainly affected by the 2- and 7-substituents of DHA. The absorbance of PhDHA-Ph beyond 400 nm is very weak. Compared with molecules with phenyl-substituted DHA (PhDHA-R), those with *N,N*-dimethyl phenyl- and biphenyl-substituted DHA exhibit a red shift and enhancement in the absorption spectra. Modification by the 4-(*N,N*-dimethyl)phenyl substituent improves the absorption. However, at the same time, the energy level of the excited state gets lower due to the rising HOMO level (Figure 3a). A short lifetime of 2.7 ns was detected (Figure 3b), which may be due to the fast nonradioactive decay caused by vibration of the *N,N*-dimethyl group. On the other hand, the diphenyl substituent can maintain the HOMO level as well as enhance absorption. As shown in Figure 3a, the extinction coefficient of DPDHA-P2F2 is nearly two times stronger than that of PhDHA-P2F2 while the emission maximum of those two photocatalysts was almost identical (Figure 3a). Different from the acceptor part attaching to the nitrogen of DHA, various substituents of the 2- and 7-sites have a minimal effect on the excited state lifetime (Figure 3b).

Redox Properties. The electrochemical and photophysical properties of photocatalysts are summarized in Table 1. The

https://dx.doi.org/10.1021/acs.macromol.0c00377
Macromolecules 2020, 53, 7053−7062

Table 2. Photo-ATRP of MMA Catalyzed by PhDHA-Ph and PhDHA-P2F

entry[a]	PC	wavelength (nm)	time (h)	conv.[b]	$M_{n,th}$[c] (kDa)	$M_{n,GPC}$[d] (kDa)	I[e]	$Đ$[d]
1	DHA-Ph	390	12	11.2%	1.1	140.3	0.008	1.78
2	DHA-P2F	390	12	89.0%	8.1	8.9	>1	1.70
3	PhDHA-Ph	390	10	65.8%	6.6	18.9	0.35	1.61
4	PhDHA-P2F	390	10	85.5%	8.6	9.4	0.91	1.40
5	PhDHA-Ph	430−440	12	20.8%	2.1	15.9	0.13	1.63
6	PhDHA-P2F	430−440	12	93.7%	9.4	15.0	0.63	1.54
7	PHDHA-P2F	455	16	77.1%	7.7	15.7	0.49	1.72

[a]Reaction conditions: Dimethyl α-bromo-α-methylmalonate (DBMM) was used as the initiator (I), the ratio of [MMA]: [I]: [PC] was 100:1:0.1, reacted at room temperatures (22−26 °C), the power of 390, 430−440, and 450 nm LED was 5, 9, and 12 W, respectively. [b]Determined by ^{1}H NMR. [c]Calculated based on conversion obtained by ^{1}H NMR (i.e., $M_{n,th} = M_{DBMM} + 100 \times \text{conversion} \times M_{MMA}$). [d]Determined by GPC in THF, based on linear PS as the calibration standard. [e]Calculated based on the $M_{n,th}$ and $M_{n,GPC}$ (i.e., $I\% = M_{n,th}/M_{n,GPC}$).

Table 3. Photo-ATRP of MMA under Visible Light by Different Photocatalysts

entry[a]	PC	wavelength (nm)	time (h)	conv.[b]	$M_{n,th}$[c] (kDa)	$M_{n,GPC}$[d] (kDa)	I[e]	$Đ$[d]
1	PhDHA-P2F2	430−440	12	87.0%	8.7	8.7	1.0	1.49
2	NPhDHA-P2F	430−440	8	62.6%	6.3	7.6	0.83	1.50
3	DPDHA-P2F2	430−440	12	90.6%	9.1	9.1	0.99	1.25
4	tBuDPDHA-P2F2	430−440	10	92.9%	9.3	12.2	0.76	1.27

[a]Reaction conditions: Dimethyl α-bromo-α-methylmalonate (DBMM) was used as the initiator (I), the ratio of [MMA]:[I]:[PC] was 100:1:0.1, reacted at room temperatures (22−26 °C), and the power of 430−440 nm LED was 12 W. [b]Determined by ^{1}H NMR. [c]Calculated based on conversion obtained by ^{1}H NMR (i.e., $M_{n,th} = M_{DBMM} + 100 \times \text{conversion} \times M_{MMA}$). [d]Determined by GPC in THF, based on linear PS as calibration standard. [e]Calculated based on the $M_{n,th}$ and $M_{n,GPC}$ (i.e., $I\% = M_{n,th}/M_{n,GPC}$).

oxidative potential $E_0(PC^{\bullet+}/PC)$ of these PCs was mainly affected by the electron density of the donor. Increasing the conjugation by modifying the diphenyl did not decrease the oxidative potential. The electron-donating substituent *N,N*-dimethyl phenyl lowered $E_0(PC^{\bullet+}/PC)$ as 0.69 V vs SCE. The reductive potential of PCs except for NPhDHA-P2F was mainly affected by the energy level of the excited state because their oxidative potential was similar. An increasing electron-withdrawing ability of the acceptor lowered the energy level of CT exited state, and the reductive ability was also reduced. Thus, PCs with two trifluoromethyl groups on the acceptor had a lower reductive potential (PhDHA-P2F2, DPDHA-P2F2, and tBuDHAPh-P2F2).

Photocatalytic ATRP. Further, we studied the photocatalyst performance in photo-ATRP of vinyl monomers. The conversion of polymerization catalyzed by DHA-Ph (Table 2, entry1) was very low, though the reaction proceeded under 390 nm irradiation. The initiator efficiency and conversion of polymerization catalyzed by DHA-P2F were much more improved compared to DHA-Ph. However, the polydispersity of the obtained polymer and such high molecular weight indicated poor control of the system (Table 2, entries 1 and 2). Without modification of the donor part (DHA), DHA-Ph and DHA-P2F were unsuitable as a photocatalyst due to the weak absorption of visible light and instability. Thus, modification of the 2- and 7-sites of DHA was necessary to enhance the absorption and stability of the photocatalyst. Both the initiator efficiency and the conversion of polymerization catalyzed by PhDHA-Ph were much higher than that of DHA-Ph (Table 2, entries 1 and 3). A lower polydispersity was also observed in the polymerization catalyzed by PhDHA-P2F compared with that catalyzed by DHA-P2F (Table 2, entries 2 and 4). On the other hand, PhDHA-P2F bearing a D−A structure performed better than PhDHA-Ph. Both the initiator efficiency and the conversion of polymerization catalyzed by PhDHA-P2F are higher than those of PhDHA-Ph under the same conditions (Table 2, entries 3 and 4 and 5 and 6). The absorption profile of PhDHA-P2F is nearly the same as that of PhDHA-Ph, which indicates that the concentration of the excited photocatalyst after excitation is approximately equal in these two systems. However, the longer excited state lifetime of PhDHA-P2F makes it more likely to reduce the initiator or C−Br bond of the dormant chain, thus contributing to a higher initiation rate. The improvement of the initiation rate could lead to an increase of the $[PC^{\bullet+}]$ concentration, and the dormancy rate mainly depends on the concentration and oxidation potential of the radical cation generated during initiation,[2,4,54,55] so rapid initiation will contribute to fast reversible dormancy and thus better controllability. Also, the CT characteristic excited state of the photocatalyst with D−A structure is beneficial for the PET process.[32] More importantly, its longer excited state lifetime results in more rapid initiation and fast dormancy, thus improving the controllability. However, the photocatalytic performance of PhDHA-P2F was better under a shorter wavelength. It is necessary to improve the photocatalysts' absorption of visible light.

First, the electron-withdrawing ability of the acceptor was enhanced by increasing the number of trifluoromethyl groups on it. Compared with PhDHA-P2F, the reduction potential of excited PhDHA-P2F2 ($E_0(PC^{\bullet+}/PC^*)$, −1.76 and −1.60 V vs SCE, respectively) and oxidation potential of its ground state ($E_0(PC^{\bullet+}/PC)$, 0.97 and 1.02 V vs SCE, respectively) were higher, thus causing the polymerization catalyzed by PHDHA-P2F2 to proceed at a slower rate as well as with a higher initiator efficiency and lower polydispersity (Table 2, entry 1). Also, NPhDHA-P2F was designed to study the effect of improving the electron-donating ability of the DHA part. Compared with PhDHA-P2F2, NPhDHA-P2F possesses a stronger absorption and lower oxidation potential $E_0(PC^{\bullet+}/PC)$ (0.69 V vs SCE), which would result in faster initiation and slower reversible dormancy, respectively. In this way, side reactions of the propagating chain radicals might be more difficult to avoid, thus resulting in poor controllability. The initiator efficiency of NPhDHA-P2F decreased when using the 430−440 nm LED

https://dx.doi.org/10.1021/acs.macromol.0c00377
Macromolecules 2020, 53, 7053−7062

Table 4. Photo-ATRP Catalyzed by DPDHA-P2F2

entry[a]	wavelength (nm)	monomer	[M]:[I]:[PC]	I	time (h)	conv.[b]	$M_{n,th}$[c] (kDa)	$M_{n,GPC}$[d] (kDa)	I[e]	$Đ$[d]
1	455	MMA	100:1: 0.1	DBMM	12	98.5%	9.9	9.9	0.99	1.43
2	430−440	MMA	100:1: 0.1	DBMM	10	90.6%	9.1	9.1	0.99	1.25
3	430−440	MMA	100:1: 0.1	EBP	10	91.2%	9.1	9.6	0.95	1.38
4	430−440	iBMA	100:1: 0.1	DBMM	10	84.7%	12.0	11.4	1.05	1.14
5	420−430	FMA	100:1: 0.1	DBMM	12	96.1%	4.8	8.9	0.53	1.56
6	430−440	MMA	100:0: 0.1	none	12	0				
7	430−440	MMA	100:1: 0	DBMM	12	9.7%				
8[e]	430−440	MMA	100:1: 0.1	DBMM	10	91.8%	9.2	10.1	0.91	1.43

[a]Reaction conditions: Dimethyl α-bromo-α-methylmalonate (DBMM) or ethyl α-bromophenylacetate (EBP) was used as the initiator (I), reacted at room temperatures (22−26 °C), and the power of 430−440 or 450 nm LED was 9 or 12 W, respectively. [b]Determined by ^{1}H NMR. [c]Calculated based on conversion obtained by ^{1}H NMR (i.e., $M_{n,th} = M_I + 100 \times \text{conversion} \times iM_M$). [d]Determined by GPC in THF, based on linear PS as a calibration standard. [e]Calculated based on the $M_{n,th}$ and $M_{n,GPC}$ (i.e., $I\% = M_{n,th}/M_{n,GPC}$). [f]Polymerization without deoxygenation.

light source for excitation (Table 3 entry 2), and there was no improvement in polydispersity observed. Also, the polymerization was stopped at the eighth hour because the color of the NPhDHA-P2F2-catalyzed system deepened when using a shorter wavelength light source (430−440 nm). Also, the color did not fade when irradiation was stopped, which indicated there might be minor deactivation of the photocatalyst. However, due to the mismatched rate of initiation and dormancy, neither PhDHA-P2F2 nor NPhDHA-P2F has a good controllability of polymerization. As mentioned above, establishing rapid equilibrium is essential for "living" photo-ATRP, which requires both rapid initiation and reversible dormancy. Thus, further modification was required to enhance absorption while maintaining the redox potential $E_0(PC^{\bullet+}/PC)$.

Thus, photocatalyst DPDHA-P2F2 was then designed to slightly strengthen the electron-withdrawing ability of the acceptor group and, more importantly, with biphenyl modification of DHA to increase absorption of visible light. As shown in Table 3 (entry 3), DPDHA-P2F2 performed better than other photocatalysts. With the optimization of the reaction conditions (Table 3, entries 1−3), the DPDHA-P2F2-catalyzed system can maintain a high initiator efficiency (0.99) and produce polymers with a low polydispersity of 1.25. In addition, the polymerization of isobutyl methacrylate (iBMA) and furfuryl methacrylate (FMA) was tested (Table 3, entries 4 and 5). What surprised us was that an even narrower polydispersity (1.14) of the polymer with high initiator efficiency was obtained in the polymerization of iBMA. Polymerization without initiator under normal conditions showed no conversion of monomer. Also, polymerization without PCs showed 10% conversion of monomer. This means that all of these components are necessary for this reaction. Monomer conversion without dioxygenation was unexpectedly as high as 91%, but polymerization was less controlled with a polydispersity of over 1.4. It is speculated that oxygen contained in the system was consumed by active species in the first stage. This stage may also cause irreversible consumption of photocatalysts, which made the polymerization less controlled. However, it was also surprising to see the high monomer conversion; we thought this may make it a potentially "air-tolerant" ATRP system, and further research will be performed. Also, tertiary butyl was further modified to increase the solubility and absorption. Modification of tertiary butyl has minor effects on the electrochemical and photophysical properties (Table 1). It is considered that the almost orthogonal position between the donor and the acceptor (Figure 5) prevents aggregation. Trifluoromethyl substituents in the acceptor may also contribute to the solubility. Thus, there was no improvement observed in the polymerization catalyzed by tBuDPDHA-P2F2 (Table 2, entry 4).

It is necessary to explain that biphenyl substitution increased the absorption by extending the π-conjugation area rather than increasing the electron-donating ability, thus maintaining the oxidation potential of the radical cation ($PC^{\bullet+}$). From the electrochemical (Figure 2d) and photochemical characterization (Figure 3a) of DPDHA-P2F2, we can see that its oxidative potential is almost the same as that of PhDHA-P2F2, while the absorption is two times stronger than that of PhDHA-P2F2. In a photo-ATRP system, the rate of initiation r_i, propagation r_p, and reversible dormancy r_d (according to a pseudotwo-body collision hypothesis[32]) can be presented as followed, Table 4. k_i, k_p, and k_d represent the corresponding rate constants[S6]

$$r_i = k_i[PC^*][R{-}Br] \tag{1}$$

$$r_p = k_p[R^\bullet] \tag{2}$$

$$r_d = k_d[R^\bullet][PC^{\bullet+}|Br^-] \tag{3}$$

The following equation can be derivated based on a steady-state assumption

$$\frac{d([R^\bullet])}{d(t)} = k_i[PC^*][R{-}Br] - k_d[R^\bullet][PC^{\bullet+}|Br^-] = 0 \tag{4}$$

Also, if ignoring the irreversible consumption of the propagating chain radical, we can reason that $[R^\bullet]$ is equal to $[PC^{\bullet+}]$. Thus, it can be presented by

$$[PC^{\bullet+}|Br^-] = [R^\bullet] = \left(\frac{k_i[PC^*][R{-}Br]}{k_d}\right)^{1/2} \tag{5}$$

$$\frac{r_d}{r_p} = \frac{k_d[PC^{\bullet+}|Br^-]}{k_p} = \left(\frac{k_d k_i[PC^*][R{-}Br]}{k_p^2}\right)^{1/2} \tag{6}$$

Also, the controllability can be semiquantitatively explained by the ratio between r_d and r_p (r_d/r_p), which indicates the competitive reaction pathways of $R^\bullet$. Therefore, it could be speculated that the larger r_d/r_p gets, the lower the possibility that irreversible chain termination could happen. From eqs 5 and 6, we can reason that the rate of both propagation and reversible dormancy would be improved when $[PC^*]$ increased, but the dormancy process would be much more accelerated, so that the

https://dx.doi.org/10.1021/acs.macromol.0c00377
Macromolecules 2020, 53, 7053−7062

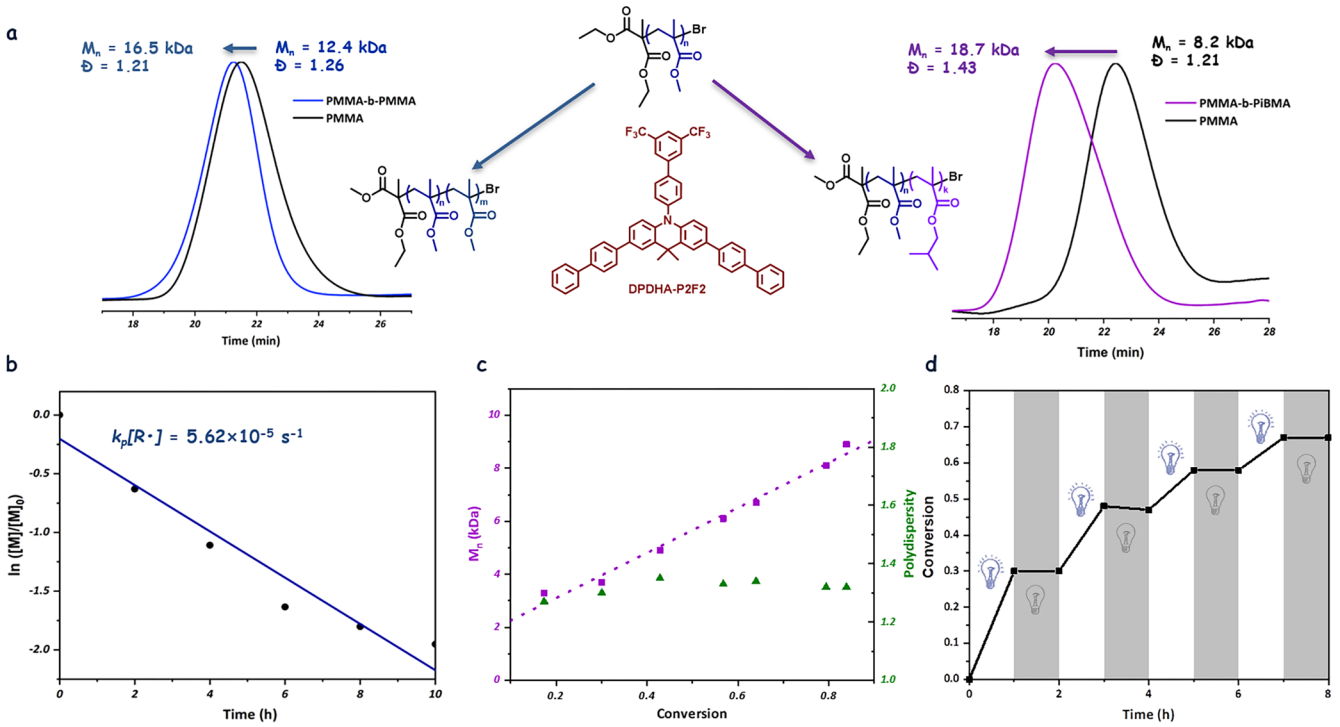

Figure 4. (a) Chain-extension polymerization from PMMA with MMA and iBMA; MI is the macroinitiator PMMA. (b) First-order kinetic plot of monomer conversion correlated with time. (c) Kinetic plot of the molecular weight and polydispersity as a function of monomer conversion. (d) Plot of monomer conversion versus time.

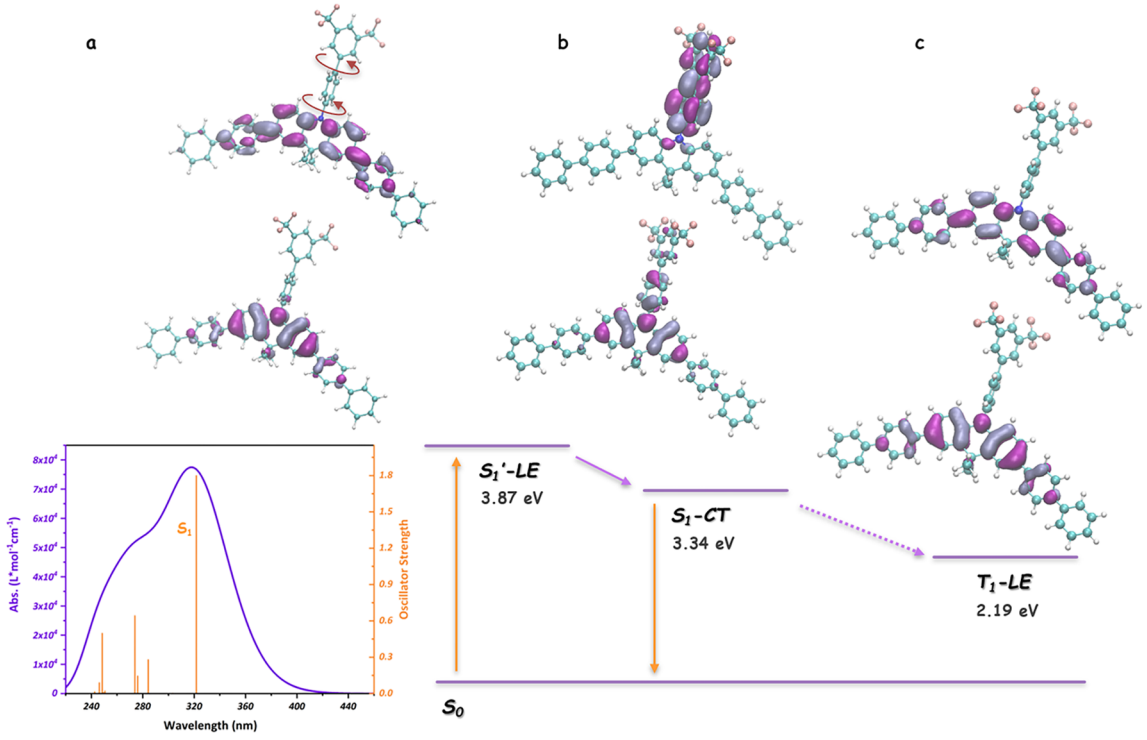

Figure 5. Excited states of DPDHA-P2F2 calculated by cam-B3LYP/6-31G(d,p) in *N*,*N*-dimethylacetamide, NTOs of the (a) S1′ excited state contributed to the vertical excitation, (b) optimized S1 excited state, and (c) optimized T1 excited state.

side reaction was reduced, which means polymerization processes would be more controllable.

Further, to measure the PET rate between PC* and initiator (DBMM), Stern−Volmer quenching experiments were also performed (SI S6). The quenching rate constants (k_q) of DPDHA-P2F2 and tBuDHA-P2F2 were 1.0×10^{10} and 1.1×10^{10} M^{-1} s^{-1}, respectively. As mentioned above, the weaker electron-donating ability contributed the higher PET rate.

https://dx.doi.org/10.1021/acs.macromol.0c00377
Macromolecules 2020, 53, 7053−7062

A chain-extension experiment was also performed to demonstrate the end-group fidelity. Block copolymers were synthesized from poly(methyl methacrylate) extended with MMA and isobutyl methacrylate (iBMA). The molecular weight increase is clearly shown in the GPC traces (Figure 4a), indicating that the macroinitiator has high retention of chain-end fidelity. The kinetics of polymerization were also studied. As shown in Figure 4b and 4c (and SI S5), a linear correlation between monomer conversion and time is observed, and polydispersity remained lower than 1.30 during the whole polymerization process. Also, a pulsed irradiation experiment (Figure 4d) was performed and showed that the polymerization was a "photocontrolled" rather "photoinduced" process.

Computational Results. To better understand the excited states probably involved in the PET process of DPDHA-P2F2, the excitation process and types of excited states were also studied by calculations. According to the computational results presented in Figure 5, absorption of DPDHA-P2F2 in vertical excitation is attributed to localized excitation (LE). This is consistent with the measured absorption of these PCs, which was barely affected by the electron-withdrawing ability of the acceptor. Afterward, through configuration change relaxation (red arrows in Figure 5a), the excited photocatalyst reaches the CT characteristic S_1 state (Figure 5b), which agrees with the broad and featureless emission profile of DPDHA-P2F2. As for the triplet excited state, the NTOs (natural transition orbitals) of the optimized T_1 state are distributed on the DHA part, which indicates its LE character. Although the distribution of the HOMO and LUMO was almost separated, the value of the calculated ΔE_{ST} was 1.25 V, which was too large to proceed with ISC or RICS like TADF dyes. Considering the lower energy level and electron distribution, it is hypothesized that it is more difficult for the T_1 state to transfer an electron to (reduce) the initiator than the S_1 state. Besides, the luminescent decay curve of DPDHA-P2F2 is single exponential, and oxygen has a minor effect on its lifetime (Table 1); thus, we assume it is S_1 that dominates the PET process.

CONCLUSION

Inspired by the strategy of designing TADF molecules, a series of organic photocatalysts bearing D−A structure was designed for photo-ATRP under visible light excitation. Different from donors with a stable oxidative state, dimethyl dihydroacridine itself is not suitable to construct a photocatalyst because of its unstable radical cation. However, we found that substitution on the active sites could stabilize the radical cation, thus allowing DHA to be the donor part of the photocatalyst for ATRP. Different modification has a significant effect on the photocatalytic performance, and with further adjustment, a well-performing photocatalyst DPDHA-P2F2 was obtained. It is notable that this strategy can probably apply to a much wider variety of electron donors, so that more structures can be used to design organic photocatalysts to gain superior performance in photoredox catalysis.

ASSOCIATED CONTENT

Supporting Information

The Supporting Information is available free of charge at https://pubs.acs.org/doi/10.1021/acs.macromol.0c00377.

Experimental procedures and characterization data for all compounds, experimental details, supplementary figures, and computation details (PDF)

AUTHOR INFORMATION

Corresponding Author

Yuguo Ma − *Beijing National Laboratory for Molecular Sciences (BNLMS), Center for Soft Matter Science and Engineering, Key Lab of Polymer Chemistry & Physics of Ministry of Education, College of Chemistry, Peking University, Beijing 100871, China;* orcid.org/0000-0002-6174-8720; Email: ygma@pku.edu.cn

Authors

Yiming Liu − *Beijing National Laboratory for Molecular Sciences (BNLMS), Center for Soft Matter Science and Engineering, Key Lab of Polymer Chemistry & Physics of Ministry of Education, College of Chemistry, Peking University, Beijing 100871, China*

Qi Chen − *Beijing National Laboratory for Molecular Sciences (BNLMS), Center for Soft Matter Science and Engineering, Key Lab of Polymer Chemistry & Physics of Ministry of Education, College of Chemistry, Peking University, Beijing 100871, China*

Yujie Tong − *Beijing National Laboratory for Molecular Sciences (BNLMS), Center for Soft Matter Science and Engineering, Key Lab of Polymer Chemistry & Physics of Ministry of Education, College of Chemistry, Peking University, Beijing 100871, China*

Complete contact information is available at: https://pubs.acs.org/10.1021/acs.macromol.0c00377

Notes

The authors declare no competing financial interest.

ACKNOWLEDGMENTS

We are thankful for support from the High-Performance Computing Platform of Peking University. This work was supported by the National Natural Science Foundation (Nos. 51573002 and 21871016) of China.

REFERENCES

(1) Ciamician, G. The photochemistry of the future. *Science (Washington, DC, U. S.)* **1912**, *36* (926), 385−394.

(2) Discekici, E. H.; Anastasaki, A.; Read de Alaniz, J.; Hawker, C. J. Evolution and Future Directions of Metal-Free Atom Transfer Radical Polymerization. *Macromolecules* **2018**, *51* (19), 7421−7434.

(3) Romero, N. A.; Nicewicz, D. A. Organic Photoredox Catalysis. *Chem. Rev.* **2016**, *116* (17), 10075−10166.

(4) Theriot, J. C.; McCarthy, B. G.; Lim, C. H.; Miyake, G. M. Organocatalyzed Atom Transfer Radical Polymerization: Perspectives on Catalyst Design and Performance. *Macromol. Rapid Commun.* **2017**, *38* (13), 1700040.

(5) Pan, X.; Fang, C.; Fantin, M.; Malhotra, N.; So, W. Y.; Peteanu, L. A.; Isse, A. A.; Gennaro, A.; Liu, P.; Matyjaszewski, K. Mechanism of Photoinduced Metal-Free Atom Transfer Radical Polymerization: Experimental and Computational Studies. *J. Am. Chem. Soc.* **2016**, *138* (7), 2411−2425.

(6) Sartor, S. M.; McCarthy, B. G.; Pearson, R. M.; Miyake, G. M.; Damrauer, N. H. Exploiting Charge-Transfer States for Maximizing Intersystem Crossing Yields in Organic Photoredox Catalysts. *J. Am. Chem. Soc.* **2018**, *140* (14), 4778−4781.

(7) Koyama, D.; Dale, H. J. A.; Orr-Ewing, A. J. Ultrafast Observation of a Photoredox Reaction Mechanism: Photoinitiation in Organocatalyzed Atom-Transfer Radical Polymerization. *J. Am. Chem. Soc.* **2018**, *140* (4), 1285−1293.

(8) Fors, B. P.; Hawker, C. J. Control of a Living Radical Polymerization of Methacrylates by Light. *Angew. Chem., Int. Ed.* **2012**, *51* (35), 8850−8853.

(9) Alfredo, N. V.; Jalapa, N. E.; Morales, S. L.; Ryabov, A. D.; Le Lagadec, R.; Alexandrova, L. Light-Driven Living/Controlled Radical

Polymerization of Hydrophobic Monomers Catalyzed by Ruthenium(II) Metalacycles. *Macromolecules* **2012**, *45* (20), 8135−8146.
(10) Pan, X.; Malhotra, N.; Zhang, J.; Matyjaszewski, K. Photoinduced Fe-Based Atom Transfer Radical Polymerization in the Absence of Additional Ligands, Reducing Agents, and Radical Initiators. *Macromolecules* **2015**, *48* (19), 6948−6954.
(11) Wu, J.; Zhang, L.; Cheng, Z.; Zhu, X. Photocatalyzed iron-based ATRP of methyl methacrylate using 1,3-dimethyl-2-imidazolidinone as both solvent and ligand. *RSC Adv.* **2017**, *7* (7), 3888−3893.
(12) Cao, Y.; Xu, Y.; Zhang, J.; Yang, D.; Liu, J. Well-controlled atom transfer radical polymerizations of acrylates using recyclable niobium complex nanoparticle as photocatalyst under visible light irradiation. *Polymer* **2015**, *61*, 198−203.
(13) Nzulu, F.; Telitel, S.; Stoffelbach, F.; Graff, B.; Morlet-Savary, F.; Lalevee, J.; Fensterbank, L.; Goddard, J.-P.; Ollivier, C. A dinuclear gold(I) complex as a novel photoredox catalyst for light-induced atom transfer radical polymerization. *Polym. Chem.* **2015**, *6* (25), 4605−4611.
(14) Guan, Z. B.; Smart, B. A remarkable visible light effect on atom-transfer radical polymerization. *Macromolecules* **2000**, *33* (18), 6904−6906.
(15) Tasdelen, M. A.; Uygun, M.; Yagci, Y. Photoinduced Controlled Radical Polymerization. *Macromol. Rapid Commun.* **2011**, *32* (1), 58−62.
(16) Ciftci, M.; Tasdelen, M. A.; Li, W.; Matyjaszewski, K.; Yagci, Y. Photoinitiated ATRP in Inverse Microemulsion. *Macromolecules* **2013**, *46* (24), 9537−9543.
(17) Pan, X.; Malhotra, N.; Simakova, A.; Wang, Z.; Konkolewicz, D.; Matyjaszewski, K. Photoinduced Atom Transfer Radical Polymerization with ppm-Level Cu Catalyst by Visible Light in Aqueous Media. *J. Am. Chem. Soc.* **2015**, *137* (49), 15430−15433.
(18) Shanmugam, S.; Boyer, C. Polymer Synthesis Organic photocatalysts for cleaner polymer synthesis. *Science* **2016**, *352* (6289), 1053−1054.
(19) You, Y.; Nam, W. Photofunctional triplet excited states of cyclometalated Ir(III) complexes: beyond electroluminescence. *Chem. Soc. Rev.* **2012**, *41* (21), 7061−7084.
(20) Singh, V. K.; Yu, C.; Badgujar, S.; Kim, Y.; Kwon, Y.; Kim, D.; Lee, J.; Akhter, T.; Thangavel, G.; Park, L. S.; Lee, J.; Nandajan, P. C.; Wannemacher, R.; Milián-Medina, B.; Lüer, L.; Kim, K. S.; Gierschner, J.; Kwon, M. S. Highly efficient organic photocatalysts discovered via a computer-aided-design strategy for visible-light-driven atom transfer radical polymerization. *Nature Catalysis* **2018**, *1* (10), 794−804.
(21) Zhao, Y.; Gong, H.; Jiang, K.; Yan, S.; Lin, J.; Chen, M. Organocatalyzed Photoredox Polymerization from Aromatic Sulfonyl Halides: Facilitating Graft from Aromatic C−H Bonds. *Macromolecules* **2018**, *51* (3), 938−946.
(22) Wu, C.; Chen, H.; Corrigan, N.; Jung, K.; Kan, X.; Li, Z.; Liu, W.; Xu, J.; Boyer, C. Computer-Guided Discovery of a pH-Responsive Organic Photocatalyst and Application for pH and Light Dual-Gated Polymerization. *J. Am. Chem. Soc.* **2019**, *141* (20), 8207−8220.
(23) Allushi, A.; Kutahya, C.; Aydogan, C.; Kreutzer, J.; Yilmaz, G.; Yagci, Y. Conventional Type II photoinitiators as activators for photoinduced metal-free atom transfer radical polymerization. *Polym. Chem.* **2017**, *8* (12), 1972−1977.
(24) Liu, X.; Zhang, L.; Cheng, Z.; Zhu, X. Metal-free photoinduced electron transfer−atom transfer radical polymerization (PET−ATRP) via a visible light organic photocatalyst. *Polym. Chem.* **2016**, *7* (3), 689−700.
(25) Kutahya, C.; Aykac, F. S.; Yilmaz, G.; Yagci, Y. LED and visible light-induced metal free ATRP using reducible dyes in the presence of amines. *Polym. Chem.* **2016**, *7* (39), 6094−6098.
(26) Allushi, A.; Jockusch, S.; Yilmaz, G.; Yagci, Y. Photoinitiated Metal-Free Controlled/Living Radical Polymerization Using Polynuclear Aromatic Hydrocarbons. *Macromolecules* **2016**, *49* (20), 7785−7792.
(27) Miyake, G. M.; Theriot, J. C. Perylene as an Organic Photocatalyst for the Radical Polymerization of Functionalized Vinyl Monomers through Oxidative Quenching with Alkyl Bromides and Visible Light. *Macromolecules* **2014**, *47* (23), 8255−8261.
(28) Kutahya, C.; Allushi, A.; Isci, R.; Kreutzer, J.; Ozturk, T.; Yilmaz, G.; Yagci, Y. Photoinduced Metal-Free Atom Transfer Radical Polymerization Using Highly Conjugated Thienothiophene Derivatives. *Macromolecules* **2017**, *50* (17), 6903−6910.
(29) Yang, L.; Huang, Y.; Peng, Y.; Liu, F.; Zhang, Q.; He, H.; Wang, J.; Jiang, L.; Zhou, Y. Pyridine-Diketopyrrolopyrrole-Based Novel Metal-Free Visible-Light Organophotoredox Catalyst for Atom-Transfer Radical Polymerization. *J. Phys. Chem. A* **2020**, *124* (6), 1068−1075.
(30) Pearson, R. M.; Lim, C.-H.; McCarthy, B. G.; Musgrave, C. B.; Miyake, G. M. Organocatalyzed Atom Transfer Radical Polymerization Using N-Aryl Phenoxazines as Photoredox Catalysts. *J. Am. Chem. Soc.* **2016**, *138* (35), 11399−11407.
(31) McCarthy, B. G.; Pearson, R. M.; Lim, C.-H.; Sartor, S. M.; Damrauer, N. H.; Miyake, G. M. Structure-Property Relationships for Tailoring Phenoxazines as Reducing Photoredox Catalysts. *J. Am. Chem. Soc.* **2018**, *140* (15), 5088−5101.
(32) Lim, C. H.; Ryan, M. D.; McCarthy, B. G.; Theriot, J. C.; Sartor, S. M.; Damrauer, N. H.; Musgrave, C. B.; Miyake, G. M. Intramolecular Charge Transfer and Ion Pairing in N,N-Diaryl Dihydrophenazine Photoredox Catalysts for Efficient Organocatalyzed Atom Transfer Radical Polymerization. *J. Am. Chem. Soc.* **2017**, *139* (1), 348−355.
(33) Theriot, J. C.; Lim, C.-H.; Yang, H.; Ryan, M. D.; Musgrave, C. B.; Miyake, G. M. Organocatalyzed atom transfer radical polymerization driven by visible light. *Science* **2016**, *352* (6289), 1082−1086.
(34) Treat, N. J.; Sprafke, H.; Kramer, J. W.; Clark, P. G.; Barton, B. E.; Read de Alaniz, J.; Fors, B. P.; Hawker, C. J. Metal-Free Atom Transfer Radical Polymerization. *J. Am. Chem. Soc.* **2014**, *136* (45), 16096−16101.
(35) Pan, X.; Fang, C.; Fantin, M.; Malhotra, N.; So, W. Y.; Peteanu, L. A.; Isse, A. A.; Gennaro, A.; Liu, P.; Matyjaszewski, K. Mechanism of Photoinduced Metal-Free Atom Transfer Radical Polymerization: Experimental and Computational Studies. *J. Am. Chem. Soc.* **2016**, *138* (7), 2411−2425.
(36) Pan, X.; Lamson, M.; Yan, J.; Matyjaszewski, K. Photoinduced Metal-Free Atom Transfer Radical Polymerization of Acrylonitrile. *ACS Macro Lett.* **2015**, *4* (2), 192−196.
(37) Uoyama, H.; Goushi, K.; Shizu, K.; Nomura, H.; Adachi, C. Highly efficient organic light-emitting diodes from delayed fluorescence. *Nature* **2012**, *492* (7428), 234−238.
(38) Chen, X.-K.; Kim, D.; Brédas, J.-L. Thermally Activated Delayed Fluorescence (TADF) Path toward Efficient Electroluminescence in Purely Organic Materials: Molecular Level Insight. *Acc. Chem. Res.* **2018**, *51* (9), 2215−2224.
(39) Adachi, C. Third-generation organic electroluminescence materials. *Jpn. J. Appl. Phys.* **2014**, *53* (6), 060101.
(40) Im, Y.; Kim, M.; Cho, Y. J.; Seo, J.-A.; Yook, K. S.; Lee, J. Y. Molecular Design Strategy of Organic Thermally Activated Delayed Fluorescence Emitters. *Chem. Mater.* **2017**, *29* (5), 1946−1963.
(41) Wong, M. Y.; Zysman-Colman, E. Purely Organic Thermally Activated Delayed Fluorescence Materials for Organic Light-Emitting Diodes. *Adv. Mater.* **2017**, *29* (22), 1605444.
(42) Yang, Z.; Mao, Z.; Xie, Z.; Zhang, Y.; Liu, S.; Zhao, J.; Xu, J.; Chi, Z.; Aldred, M. P. Recent advances in organic thermally activated delayed fluorescence materials. *Chem. Soc. Rev.* **2017**, *46* (3), 915−1016.
(43) Zhang, Q.; Li, B.; Huang, S.; Nomura, H.; Tanaka, H.; Adachi, C. Efficient blue organic light-emitting diodes employing thermally activated delayed fluorescence. *Nat. Photonics* **2014**, *8* (4), 326−332.
(44) Cai, X.; Gao, B.; Li, X.-L.; Cao, Y.; Su, S.-J. Singlet-Triplet Splitting Energy Management via Acceptor Substitution: Complanation Molecular Design for Deep-Blue Thermally Activated Delayed Fluorescence Emitters and Organic Light-Emitting Diodes Application. *Adv. Funct. Mater.* **2016**, *26* (44), 8042−8052.
(45) Wada, Y.; Kubo, S.; Kaji, H. Adamantyl Substitution Strategy for Realizing Solution-Processable Thermally Stable Deep-Blue Thermally Activated Delayed Fluorescence Materials. *Adv. Mater.* **2018**, *30* (8), 1705641.

https://dx.doi.org/10.1021/acs.macromol.0c00377
Macromolecules 2020, 53, 7053−7062

(46) Lin, T. A.; Chatterjee, T.; Tsai, W. L.; Lee, W. K.; Wu, M. J.; Jiao, M.; Pan, K. C.; Yi, C. L.; Chung, C. L.; Wong, K. T.; Wu, C. C. Sky-Blue Organic Light Emitting Diode with 37% External Quantum Efficiency Using Thermally Activated Delayed Fluorescence from Spiroacridine-Triazine Hybrid. *Adv. Mater.* **2016**, *28* (32), 6976−6983.
(47) Zhang, Q.; Tsang, D.; Kuwabara, H.; Hatae, Y.; Li, B.; Takahashi, T.; Lee, S. Y.; Yasuda, T.; Adachi, C. Nearly 100% internal quantum efficiency in undoped electroluminescent devices employing pure organic emitters. *Adv. Mater.* **2015**, *27* (12), 2096−2100.
(48) Numata, M.; Yasuda, T.; Adachi, C. High efficiency pure blue thermally activated delayed fluorescence molecules having 10H-phenoxaborin and acridan units. *Chem. Commun.* **2015**, *51* (46), 9443−9446.
(49) Lee, J.; Aizawa, N.; Numata, M.; Adachi, C.; Yasuda, T. Versatile Molecular Functionalization for Inhibiting Concentration Quenching of Thermally Activated Delayed Fluorescence. *Adv. Mater.* **2017**, *29* (4), 1604856.
(50) Andrew, T. L.; Swager, T. M. Detection of explosives via photolytic cleavage of nitroesters and nitramines. *J. Org. Chem.* **2011**, *76* (9), 2976−2993.
(51) Buss, B. L.; Lim, C.-H.; Miyake, G. M. Dimethyl Dihydroacridines as Photocatalysts in Organocatalyzed Atom Transfer Radical Polymerization of Acrylate Monomers. *Angew. Chem., Int. Ed.* **2020**, *59* (8), 3209−3217.
(52) Sun, D.; Rosokha, S. V.; Kochi, J. K. Donor-acceptor (electronic) coupling in the precursor complex to organic electron transfer: Intermolecular and intramolecular self-exchange between phenothiazine redox centers. *J. Am. Chem. Soc.* **2004**, *126* (5), 1388−1401.
(53) Odom, S. A.; Ergun, S.; Poudel, P. P.; Parkin, S. R. A fast, inexpensive method for predicting overcharge performance in lithium-ion batteries. *Energy Environ. Sci.* **2014**, *7* (2), 760−767.
(54) Matyjaszewski, K. Atom Transfer Radical Polymerization (ATRP): Current Status and Future Perspectives. *Macromolecules* **2012**, *45* (10), 4015−4039.
(55) Tasdelen, M. A.; Uygun, M.; Yagci, Y. Photoinduced Controlled Radical Polymerization in Methanol. *Macromol. Chem. Phys.* **2010**, *211* (21), 2271−2275.
(56) Matyjaszewski, K.; Xia, J. Atom Transfer Radical Polymerization. *Chem. Rev.* **2001**, *101* (9), 2921−2990.

https://dx.doi.org/10.1021/acs.macromol.0c00377
Macromolecules 2020, 53, 7053−7062